

Studies on the photodissociation and symmetry of $\text{SO}_2^+(\tilde{D})$

Limin Zhang,^{a)} Zhong Wang, Jiang Li, Feng Wang, Shilin Liu, Shuqin Yu,
and Xingxiao Ma

Laboratory of Bond Selective Chemistry, Department of Chemical Physics, University of Science
and Technology of China, Hefei, Anhui 230026, People's Republic of China

(Received 8 January 2003; accepted 27 February 2003)

With the preparing of $\text{SO}_2^+(\tilde{X}^2A_1(000))$ by $[3+1]$ multiphoton ionization of the neutral SO_2 molecules at 380.85 nm, the photodissociation process and the symmetry of the excited states \tilde{D} of SO_2^+ molecular ions has been investigated by measuring the photofragment SO^+ excitation (PHOFEX) spectrum in ultraviolet (282–332 nm) and in visible (562–664 nm) wavelength ranges, respectively. The $\tilde{D}(v_100)$, $\tilde{D}(0v_20) \leftarrow \tilde{X}^2A_1(000)$ transitions of SO_2^+ were assigned in the PHOFEX spectrum in the UV range. By comparing the discernible PHOFEX spectrum in UV range with the continuous PHOFEX spectrum in visible range, it is deduced that (i) around $\text{SO}_2^+(\tilde{D})$ there exists a repulsive state α^2A_2 converging to the dissociation limit of $\text{SO}^+(X^2\Pi) + \text{O}(^3P_g)$, (ii) the coupling between $\text{SO}_2^+(\tilde{D})$ and $\text{SO}_2^+(\alpha^2A_2)$ leads to the dissociation to $\text{SO}^+(X^2\Pi) + \text{O}(^3P_g)$, (iii) the symmetry of \tilde{D} state is \tilde{D}^2B_1 . © 2003 American Institute of Physics.
[DOI: 10.1063/1.1568728]

I. INTRODUCTION

The studies of photodissociation dynamics of molecules (including molecular ions) can provide useful information on the interaction between the electronic states of molecules, and the breaking of bonds to form fragment products, etc.^{1,2} The development of sophisticated new experimental methods, such as the use of multicolor lasers, supersonic molecular beams, and the time-of-flight (TOF) mass spectroscopy, has made it possible to study the photofragmentation mechanism of unstable molecules (free radicals, molecular ions) in unprecedented precision (high resolution spectra and mass selected).^{3,4}

SO_2 and the ions derived from it could play important roles in atmospheric chemistry, environmental pollution, and industry, such as in the overall chemistry of the dry etching process.^{5,6} To obtain the spectral data and to learn the dissociation dynamics of SO_2^+ , the photoelectron spectroscopy with molecular beam,^{7,8} the electron impact ionization,⁹ and the photoionization^{10,11} of SO_2 molecule were recently used. The common ground of the above-mentioned methods is to excite the neutral molecule SO_2 by using high energy photons or electrons. The only available photodissociation spectrum of SO_2^+ ion by direct photoexcitation of SO_2^+ itself, as known by us, was from Thomas *et al.*¹² In their study, the SO_2^+ ions prepared by electron impact were selected by a triple quadrupole system and the photodissociation spectrum of SO_2^+ ion was obtained by the coaxial irradiation of tunable dye laser. However, the signal-to-noise ratio and resolution for their photodissociation spectra of SO_2^+ ion seems poor.

The motivation of this work is to learn the predissociation mechanisms of $\text{SO}_2^+(\tilde{E}, \tilde{D}, \tilde{C})$, which overlap each other

and are located at the third complex photoelectron band of SO_2 .^{7,8} Similar to our previous study on the photofragment excitation (PHOFEX) spectrum of CS_2^+ ,³ in this study a two color method is used to obtain the PHOFEX spectrum of SO_2^+ . That is, the SO_2^+ ions were prepared by the $[3+1]$ resonantly enhanced multiphoton ionization (REMPI) of neutral SO_2 molecules at 380.85 nm, the photofragment SO^+ excitation (PHOFEX) spectrum of SO_2^+ ion was obtained by scanning the second tunable pulsed laser in the range of 281–334 nm (UV) and 562–668 nm (visible), respectively. From the UV and visible PHOFEX spectra, the symmetry and the predissociation of $\text{SO}_2^+(\tilde{D})$ have been studied.

II. EXPERIMENT

The experimental setup is similar to that reported previously.^{3,13} Briefly it consists of (i) a pulsed molecular beam source to generate the jet-cooled SO_2 molecules, (ii) two dye laser systems pumped simultaneously by Nd:yttrium-aluminum-garnet (YAG) lasers, and (iii) a home-made TOF mass spectrometer.

The jet-cooled SO_2 molecules were produced by the supersonic expansion of a SO_2/He gas mixture ($\text{SO}_2/\text{He} \sim 20\%$) through a pulsed nozzle (General Valve) with a nozzle orifice diameter of 0.5 mm into a photoionization chamber. The laser-molecule interaction region was located 6 cm downstream from the nozzle orifice. The time-of-flight mass spectrometer was pumped by two turbomolecular pumps of 500 and 450 l/s. The stagnation pressure was kept at around 3 atm, and the operating pressures in the interaction region was 2×10^{-5} Torr.

One dye laser FL3002 (Lambda Physics), pumped by the THG (354.7 nm) output of a Nd:YAG laser (LABest Optronics), was used for photoionization. The second dye laser HD-500 with frequency doubling HD-1000 (Lumonics), pumped

^{a)} Author to whom all correspondence should be addressed. Electronic mail: Imzha@ustc.edu.cn

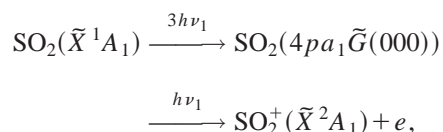
by the SHG (532 nm) output a Nd:YAG laser GCR-170 (Spectra-Physics), was used for photodissociation. The output of photoionization dye laser (380.85 nm, ~ 1.5 mJ/pulse) was focused perpendicularly on the molecular beam of SO_2 by a quartz lens with $f=120$ mm and was used to prepare SO_2^+ molecular ions via $[3+1]$ REMPI of SO_2 .¹⁴ The photodissociation dye laser, with the output of ~ 0.1 mJ/pulse in the range of 281–332 nm and ~ 1.2 mJ/pulse in the range of 562–664 nm, was employed to dissociate SO_2^+ ions via one-photon and two-photon excitation, respectively. This light was coaxially counterpropagated with the photoionization laser, and focused by another quartz lens with $f=500$ mm (for 281–332 nm) and $f=300$ mm (for 562–664 nm), respectively. Both dye lasers were temporally and spatially matched with each other at the laser–molecular interaction point. The wavelength of laser was calibrated by Ne hollow cathode lamp.

The produced ions, including the parent SO_2^+ ions and the fragment ions, were extracted and accelerated into a TOF mass spectrometer and drifted along a 70-cm-long TOF tube, and finally detected by a microchannel plate (MCP) detector. The signals from the MCP output were amplified with a pre-amplifier (NF, BX-31), and the mass-resolved data were collected by averaging the amplified signals for selected mass species with boxcar averages (Stanford SR250), then interfaced to a PC for data storage.

III. RESULTS AND DISCUSSION

A. The preparation of SO_2^+

The ionization potential of SO_2 molecule is 12.35 eV.^{7,8} The $[3+1]$ REMPI spectrum of SO_2 molecule in the range of 365–405 nm has been studied in detail.^{13,14} The resonance band located at $\lambda=380.85$ nm was used in this study owing to the dominating parent ion SO_2^+ and very few fragment ions SO^+ and S^+ at this wavelength. So we could certainly prepare almost exclusive SO_2^+ ions with minimum amount of SO^+ and S^+ ions by using a lens with middle focus length ($f=120$ mm) and optimizing the pulse energy of the ionization laser at ~ 1.5 mJ, as shown in the TOF mass spectrum of Fig. 1(a) where the amounts of SO^+ and S^+ ions are less than 1/15 of SO_2^+ . The $[3+1]$ REMPI of SO_2 at $\lambda_1=380.85$ nm can be expressed as



where $4pa_1\tilde{G}$ represents the \tilde{G} state with a Rydberg orbital of $4pa_1$. The \tilde{G} Rydberg state with the A_1 symmetry converges to the SO_2^+ ground state (\tilde{X}^2A_1).¹⁴ Though the 13.00 eV energy of four photon with $\lambda_1=380.85$ nm can excite $\text{SO}_2(\tilde{X}^1A_1)$ to a position just above $\text{SO}_2^+(\tilde{A}^2A_2)$ at 12.99 eV, the population of $\text{SO}_2^+(\tilde{A}^2A_2)$ can be omitted, at least, owing to the unfavorable transition from $\text{SO}_2(\tilde{G}A_1)$ to $\text{SO}_2^+(\tilde{A}^2A_2)$.

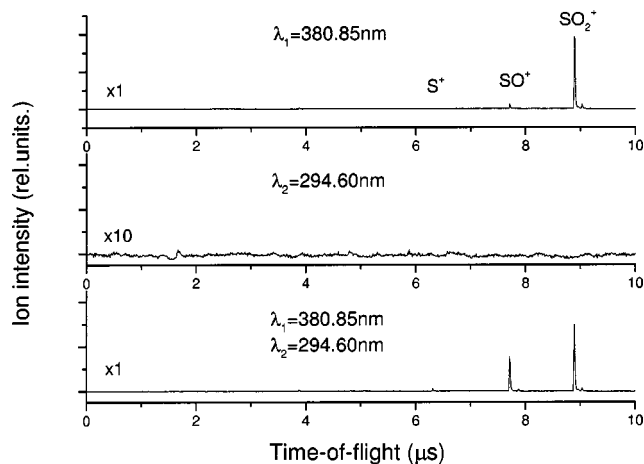


FIG. 1. The TOF mass spectra averaged over 256 laser shots and obtained with (a) only the photoionization laser at 380.85 nm, (b) only the photodissociation laser at 294.60 nm, and (c) both the photoionization laser and the dissociation laser overlapped spatially and temporally with each other. The SO_2^+ ions in (a) and (c) were generated via $[3+1]$ REMPI of SO_2 molecules by the ionization laser, and the SO^+ ions in (c) were produced from the dissociation of SO_2^+ ions by the dissociation laser. The pulse energies of the ionization laser and the dissociation laser were optimized and maintained at 1.5 and 0.1 mJ, respectively.

B. UV photofragment SO^+ excitation spectrum

By carefully controlling the intensity of the dissociation laser, no ion signal could be observed only with this laser as shown in Fig. 1(b) at $\lambda_2=294.6$ nm, but the remarkably strong SO^+ signal appeared in TOF mass spectrum with both the ionization laser and the dissociation laser as shown in Fig. 1(c). The SO^+ ions were confirmed to be generated completely from the interaction of the dissociation laser on the parent molecular SO_2^+ ions, by varying the temporal delay and the spatial overlap between the two lasers. To avoid the disturbance from autoionization of neutral SO_2 , there was about 60 ns delay temporally and slight separation in the direction of ion flight between the dissociation laser and the ionization laser in the laser–molecular interaction region.

Figures 2(a)–2(d) show the PHOFEX spectrum obtained in the wavelength range of 282–334 nm with the ionization laser fixed at 380.85 nm. In the entire scan range the signal of SO^+ ion is dominated compared to the very weak S^+ ion signal. The discernible resonance bands are shown in the PHOFEX spectrum by measuring SO^+ .

From the spectroscopic data obtained from the photoelectron spectroscopy of SO_2 ,^{7,8} it is known that the $\text{SO}_2^+(\tilde{E}, \tilde{D}, \tilde{C}) \leftarrow \text{SO}_2^+(\tilde{X}^2A_1)$ transitions are allowed and can be excited by one photon in the wavelength range of 291–312 nm,¹⁵ where \tilde{E} , \tilde{D} , \tilde{C} , possess 2B_2 , 2B_1 , and 2A_1 symmetry, respectively. Notice that we write \tilde{E} , \tilde{D} , \tilde{C} states just according to the energy position from high to low and leave their symmetry assignment as a problem to be discussed next. The dependence of SO^+ ionic signal on dissociation laser intensity in a log–log plot is shown in Fig. 3 where the ionization laser and dissociation laser are fixed at 380.85 and 306.36 nm, respectively. The slope of the line for SO^+ signal is about 0.8 by least-squares fitting. This supports that the SO^+ signal was from one-photon excitation of SO_2^+ .

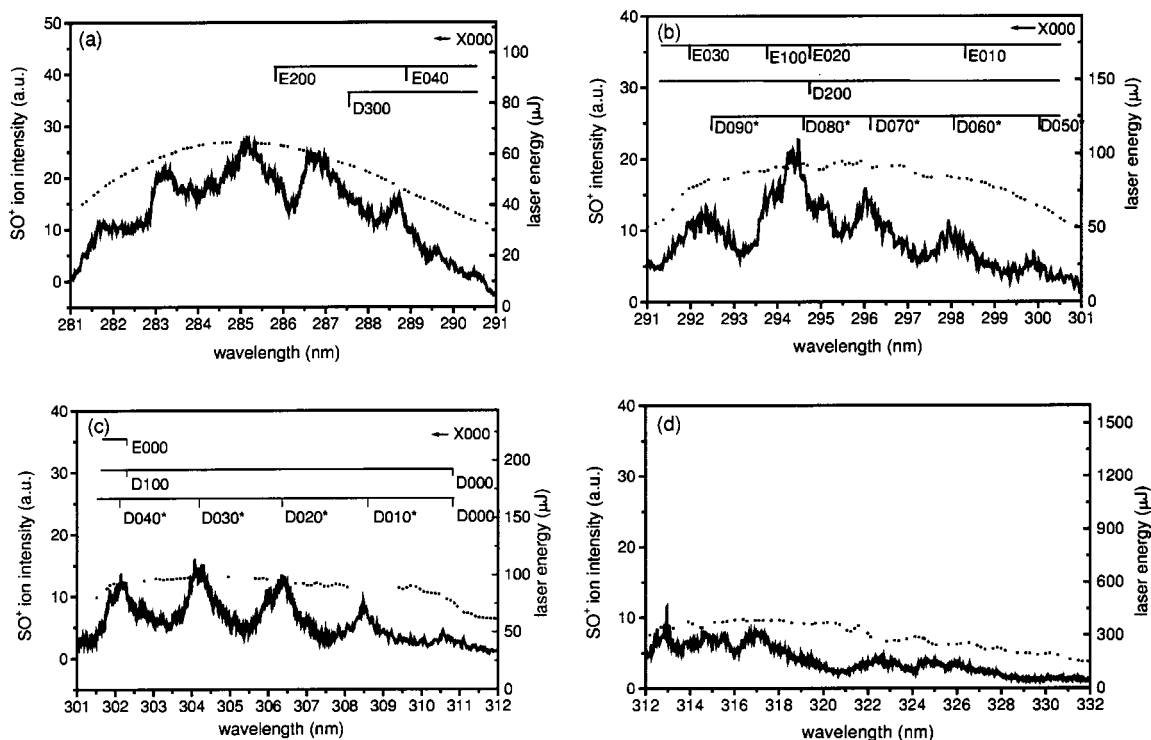


FIG. 2. The PHOFEX spectrum of SO_2^+ obtained by monitoring SO^+ ions in the wavelength range of 292–334 nm. New assignment to bend vibration of \tilde{D} state was marked with an asterisk, other assignments were given by referring to the photoelectron spectra of Ref. 8. The laser efficiency curve was given at the top of spectra in (a)–(d). The average intensity of dissociation laser increases from (a) to (d).

The possible assignments for the PHOFEX spectrum were tried, and it is found that if only to assign the PHOFEX spectrum to the transitions from the vibration level (000) of $\text{SO}_2^+(\tilde{X}^2A_1)$ that the complete vibration series could be obtained for the PHOFEX spectrum, as shown in Fig. 2 and Table I. This proves that in the $[3+1]$ REMPI of SO_2 the excited $\text{SO}_2(4p\alpha_1\tilde{G}(000))$ converges to $\text{SO}_2^+(\tilde{X}^2A_1(000))$ finally.

The assignments of \tilde{D} ($v_1=0-3, v_2=0, v_3=0$) $\leftarrow \tilde{X}^2A_1(000)$ and \tilde{E} ($v_1=0-2, v_2=0-4, v_3=0$) $\leftarrow \tilde{X}^2A_1(000)$ of SO_2^+ were deduced from the data of pho-

toelectron spectra¹² and was shown in Fig. 2. Although the transition of $\text{SO}_2^+(\tilde{C}) \leftarrow \text{SO}_2^+(\tilde{X}^2A_1)$ is allowed, it was hard to find the resonance band series in the PHOFEX spectrum.

It is very interesting that the three resonance bands with the adjacent space of $\sim 230 \text{ cm}^{-1}$, located at 304.20, 306.36, and 308.60 nm, respectively, cannot be assigned reasonably

TABLE I. Band positions and assignments for the fragment SO^+ excitation spectrum of SO_2^+ .

Transition of SO_2^+ $\leftarrow \tilde{X}^2A_1(000)$	λ_{exp} (nm)	$\lambda_{\text{exp}} - \lambda_{\text{PES}}$ (nm) ^a	Transition of SO_2^+ $\leftarrow \tilde{X}^2A_1(000)$	λ_{exp} (nm)	Spacing (cm^{-1})
$\tilde{E}^2B_2(v_1v_2v_3)$					
000	302.12	-0.18	010	308.60	0
010	298.06	-0.26	020	306.36	231.4
020	294.60	-0.14	030	304.20	236.9
100	293.84	0.08	040	302.12	231.8
030	292.00	0.03	050	300.03	226.3
040	288.79	-0.10	060	298.06	230.6
200	285.35	-0.35	070	296.14	220.3
			080	294.60	217.5
$\tilde{D}^2B_1(v_100)$					
000	310.68	-0.14	090	292.48	210.0
100	302.12	-0.18			
200	294.60	-0.14			
300	287.29	-0.26			

^a λ_{exp} is measured by us and λ_{PES} is from the photoelectron spectra of Ref. 8.

^bNo PES data.

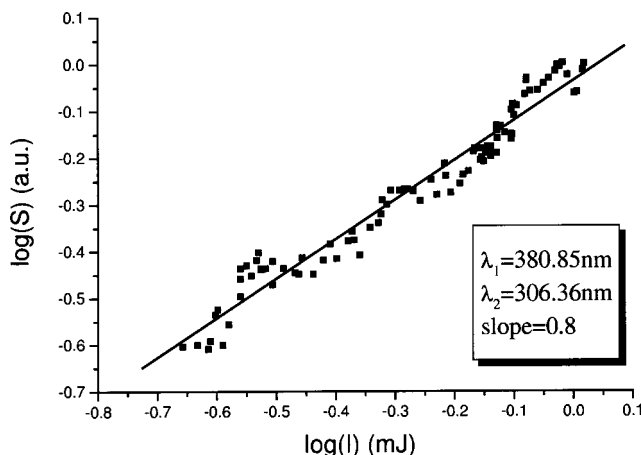


FIG. 3. Dependence of SO^+ ion signal on laser intensity in double logarithmic form obtained with $\lambda_1=380.85 \text{ nm}$ and $\lambda_2=306.36 \text{ nm}$ for ionization laser and dissociation laser, respectively. The slope of regression line is 0.8.

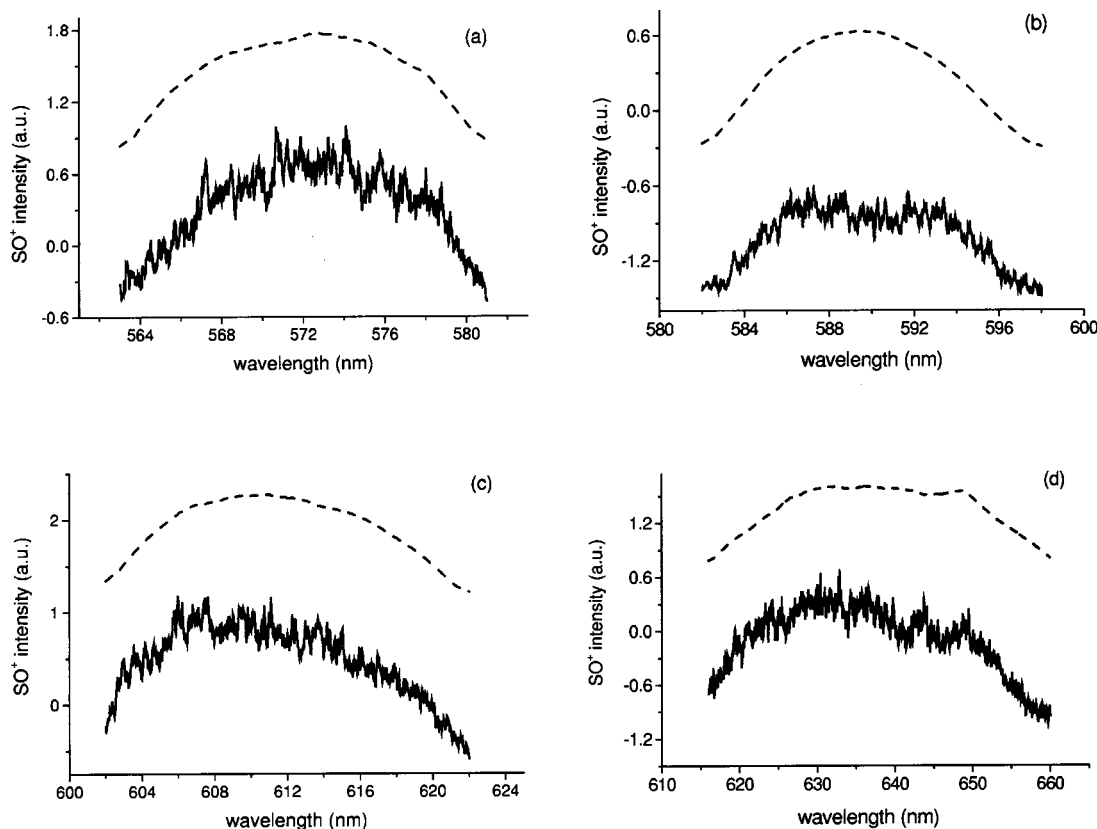


FIG. 4. The PHOFEX spectrum of SO_2^+ was obtained by monitoring SO^+ ions in the wavelength range of 563–660 nm. The laser efficiency curve was given at the top of spectra in (a)–(d). The excited spectrum of SO^+ ions had no clear resonant structure.

by using the available spectral data of SO_2^+ .^{7,8} Owing to the energy positions of these bands being between $\text{SO}_2^+(\tilde{D}(000))$ and $\text{SO}_2^+(\tilde{E}(000))$, it is reasonable to assign these bands to the transitions of $\tilde{D}(0\nu_2 0) \leftarrow \tilde{X}^2A_1(000)$ for SO_2^+ , where ν_2 is the bend vibration quantum numbers. The important support for this assignment is the large change of molecular bond angle from 136.5° of $\text{SO}_2^+(\tilde{X}^2A_1)$ to 119.5° of $\text{SO}_2^+(\tilde{D})$,¹⁶ which is favorable to excite the transition to the bent vibration levels of $\text{SO}_2^+(\tilde{D})$ from $\text{SO}_2^+(\tilde{X}^2A_1)$. The bend vibration excitation of $\text{SO}_2^+(\tilde{D})$ was not given in photoelectron spectrum,^{7,8} maybe owing to the nearly same molecular bond angle of 119.5° for $\text{SO}_2^+(\tilde{D})$ and $\text{SO}_2(\tilde{X}^1A_1)$,¹⁶ which is unfavorable to excite the bent vibration mode of $\text{SO}_2^+(\tilde{D})$ from $\text{SO}_2(\tilde{X}^1A_1)$. Following this assignment, the bend vibration levels from $\nu_2=0$ to $\nu_2=9$ of $\text{SO}_2^+(\tilde{D}(0\nu_2 0))$ were obtained, as shown in Fig. 2. New harmonic bend vibrational frequency $\nu_2=241.78 \pm 0.92 \text{ cm}^{-1}$ and the anharmonicity constants $X_{22}=-1.71 \pm 0.01 \text{ cm}^{-1}$ for $\text{SO}_2^+(\tilde{D})$ were deduced by using least-squares fitting. The lower ν_2 of $\sim 240 \text{ cm}^{-1}$ for the \tilde{D} state, given by us, in comparison with ν_2 of $\sim 360 \text{ cm}^{-1}$ for the \tilde{C} state, given by the photoelectron spectrum,^{7,8} means that the potential curve of the \tilde{D} state is not similar to other states along the bend vibrational coordinate, further studies both in experiment and in theory are needed. We also tried to assign in the PHOFEX spectrum the sum frequency excitation of ν_1 and ν_2 of the \tilde{D} state, such as

$\tilde{D}(110)$, $\tilde{D}(210)$, etc., unfortunately the diffusion of the spectrum prevented us from getting precise assignment to them, so that no sum frequency was shown in Fig. 2.

C. Visible photofragment SO^+ excitation spectrum

To learn the predissociation process of $\text{SO}_2^+(\tilde{D})$ two photon transitions of $\text{SO}_2^+(\tilde{X}^2A_1)$ in the range of 562–668 nm, by which the energy position of $\text{SO}_2^+(\tilde{D})$ can be reached, were completed. The continuous PHOFEX spectrum without discernible band structure in this visible range was obtained by measuring SO^+ , as shown in Fig. 4. It is reasonable to assume that there should be a repulsive state converging to $\text{SO}^+(X^2\Pi) + \text{O}(^3P_g)$, by which the continuous PHOFEX spectrum excited by two photons can be produced. Next we will consider the symmetry of this repulsive state around the \tilde{D} state, if it exists. For the molecule with C_{2v} point group symmetry, like SO_2^+ , the transition of 2B_1 , 2A_1 , $^2B_2 \leftarrow \tilde{X}^2A_1$ is allowed, but the transition of $^2A_2 \leftarrow \tilde{X}^2A_1$ is forbidden¹⁵ for one photon excitation. However, the transitions both of 2B_1 , 2A_1 , $^2B_2 \leftarrow \tilde{X}^2A_1$ and of $^2A_2 \leftarrow \tilde{X}^2A_1$ are allowed for two photon excitation. Notice that the energy position, reached either by one photon excitation of 281–332 nm laser or by two photon excitation of 562–664 nm laser, should be the same, when $\text{SO}_2^+(\tilde{X}^2A_1)$ was excited. Thus, the similar PHOFEX spectrum should be obtained by using 281–332 nm laser or by using 562–664 nm

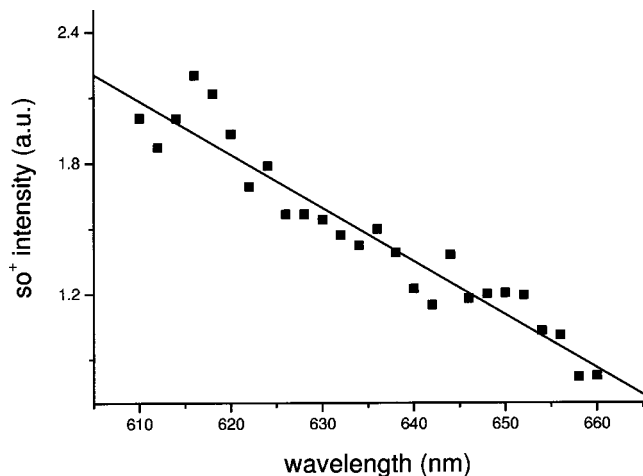


FIG. 5. The distribution of the SO^+ ion intensity is obtained by monitoring SO^+ ions in the wavelength range of 610–660 nm. The fluctuant influence of dissociation laser energy has been deducted.

laser, if there is only 2B_1 , 2A_1 , ${}^2B_2 \leftarrow \tilde{X}{}^2A_1$ transitions. However, the obvious resonance band structure appeared in the PHOFEX spectrum of 281–332 nm and the continuum appeared in the PHOFEX spectrum of 562–664 nm, as shown in Figs. 2 and 4. Considering that the rate of direct dissociation via a repulsive state is much greater than the rate of predissociation of a bound state, it is reasonably suggested that there should be a repulsive state of 2A_2 symmetry around \tilde{D} states, which is allowed for two photon excitation and is forbidden for one photon excitation from $\tilde{X}{}^2A_1$. We call this supposed repulsive state $\alpha{}^2A_2$. The efficiency of the SO^+ ion yield in the wavelength range of 610–660 nm is shown in Fig. 5. In fact, it provides evidence of the existence of a repulsive state by the decreasing SO^+ ion yield with increasing wavelength. Of course, support from theoretical calculation is needed for the suggestion that $\alpha{}^2A_2$ is a repulsive state. Although the two photon transition in the range of 562–664 nm could excite $\text{SO}_2^+(\tilde{X}{}^2A_1)$ into the 2B_1 , 2A_1 , 2B_2 states correlated to \tilde{E} , \tilde{D} , \tilde{C} , the direct dissociation rate via $\alpha{}^2A_2$ repulsive state excited by two photon transition will be much larger than the predissociation rate via 2B_1 , 2A_1 , 2B_2 states correlated to \tilde{E} , \tilde{D} , \tilde{C} ,¹⁰ and the total effect will be like the direct dissociation. Thus, it is not surprising that only the continuous PHOFEX spectrum without discernible resonance band structure was obtained by using two photon transition in the range of 562–664 nm. Notice that if the “pure” two photon transition in the range of 562–664 nm is replaced by $[1+1]$ transition via the congested vibration levels of the $\tilde{B}{}^2B_2$ state,^{7,8} the above-presented discussion is still effective. The dependence of SO^+ ionic signal on dissociation laser intensity in a log–log plot is shown in Fig. 6 where the ionization laser and dissociation laser are fixed at 380.85 and 578 nm, respectively. The slope of the line for the SO^+ signal is about 0.99 by least-squares fitting. This indicates that the PHOFEX spectrum in the range of 562–664 nm is indeed from the $[1+1]$ transition via the congested vibration levels of the $\tilde{B}{}^2B_2$ state and the first step of transitions is saturated.

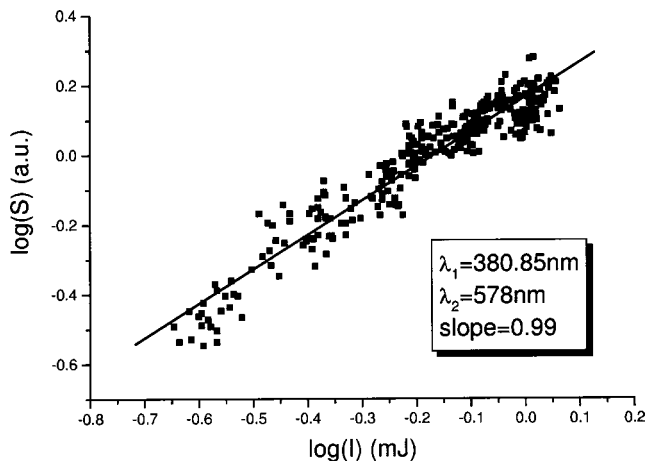


FIG. 6. Dependence of SO^+ ion signal on laser intensity in double logarithmic form obtained with $\lambda_1 = 380.85$ nm and $\lambda_2 = 578$ nm for ionization laser and dissociation laser, respectively. The slope of regression line is 0.99.

D. The symmetry and the predissociation mechanism of excited states \tilde{D}

The symmetry of \tilde{E} , \tilde{D} , \tilde{C} is still an arguable problem, although they were denoted as $\tilde{E}{}^2B_1$, $\tilde{D}{}^2A_1$, $\tilde{C}{}^2B_2$, respectively, in several references.^{7,8,10} For example, according to the results of *ab initio* self-consistent field calculations by Hillier and Saunders,¹⁶ the three electronic states located at 16.50, 16.34, and 15.90 eV, respectively, should be denoted as $\tilde{E}{}^2B_2$, $\tilde{D}{}^2A_1$, $\tilde{C}{}^2B_1$. Thomas *et al.*¹² questioned the assignment of $\tilde{D}{}^2A_1$, and proposed the assignment of $\tilde{D}{}^2B_2$ and the possible assignment of $\tilde{C}{}^2B_1$.

On the other hand, it is known that \tilde{E} , \tilde{D} , \tilde{C} states could predissociate to the first limit to produce fragment ion SO^+ .^{7–11,17} However, the detailed predissociation mechanism of \tilde{E} , \tilde{D} , \tilde{C} is still not clear, such as which kind of repulsive state could be coupled to \tilde{E} , \tilde{D} , \tilde{C} states in the predissociation process. Dujardin and Leach¹⁰ suggested that the products $\text{SO}^+(X{}^2\Pi) + \text{O}({}^3P_g)$ could combine to form a repulsive state with the symmetry of 2B_2 , called $\beta{}^2B_2$, and the state $\tilde{C}{}^2B_2$ coupled to it to produce predissociation. $\text{SO}^+(X{}^2\Pi) + \text{O}({}^3P_g)$ can also combine to form a repulsive state of 2B_1 , and the state $\tilde{E}{}^2B_1$ coupled to it to produce the homogeneous predissociation. Unfortunately, these suggested repulsive states have not received further support either from the theoretical calculation or from the experimental evidence.

In this work, the main vibrational series observed in UV range was from the $\tilde{D} \leftarrow \tilde{X}{}^2A_1(000)$ transition of SO_2^+ , although the $\tilde{E}(v_1=0-2, v_2=1-4, v_3=0) \leftarrow \tilde{X}{}^2A_1(000)$ transition could not be excluded as shown above. In the UV PHOFEX spectrum of $\tilde{D} \leftarrow \tilde{X}{}^2A_1(000)$, the character of the predissociation was shown, such as the resonance bands have no resolved rotational structure. To explain the one photon PHOFEX spectrum of SO_2^+ in UV range, the predissociation mechanism of \tilde{D} bound state need to be considered. Owing to the fact that the \tilde{D} state belongs to one of the 2B_1 , 2A_1 , 2B_2 bound states, it could not couple to the $\alpha{}^2A_2$ repulsive

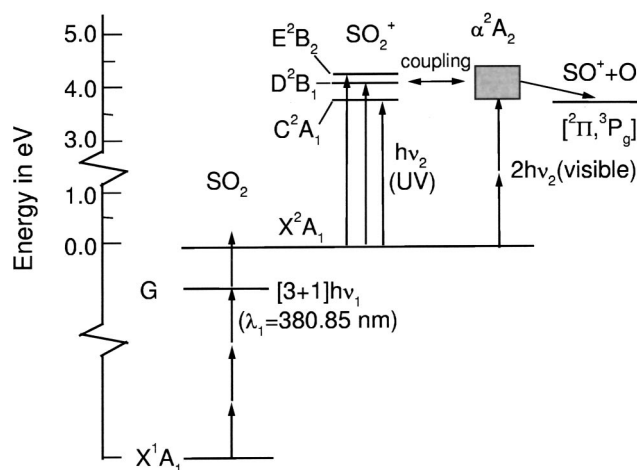
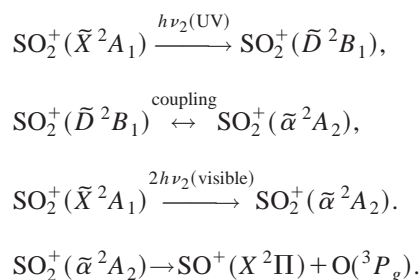


FIG. 7. Schematic energy level diagram (Refs. 7, 8, 12, and 14) of SO_2^+ with possible interaction among the electronic states to illustrate the excitation and dissociation processes. The symmetry assignments of $\tilde{E}, \tilde{D}, \tilde{C}$ states of SO_2^+ are modified by us.

state by electron–electron interaction, but the coupling by electron–vibration interaction between the \tilde{D} state and α^2A_2 repulsive state is possible. SO_2^+ is a triple atomic planar molecule ion with C_{2v} point group symmetry, $C_2(z)$, and the molecular axis along the y coordinate in the molecular plane. The possible vibrational mode could be that of a_1 and b_2 symmetry and the impossible vibration modes are that of b_1 and a_2 symmetry which need to change symbol for the nucleus reverse about molecular plane.¹⁵ If the direct product of the \tilde{D} electronic state and vibration a_1 and b_2 contains α^2A_2 symmetry, then the coupling between the electronic states among \tilde{D} and the α^2A_2 repulsive state via electron vibration interaction is possible. Obviously, only the \tilde{D} state with 2B_1 symmetry satisfies the above-mentioned condition ($B_1 \times b_2 = A_2$) and can couple to the α^2A_2 repulsive state via electron vibration interaction. Thus, the symmetry of the \tilde{D} state is determined as 2B_1 and \tilde{D}^2B_1 predissociate to $\text{SO}^+(X^2\Pi) + \text{O}(^3P_g)$ by coupling to α^2A_2 repulsive state via electron vibration interaction.

Figure 7 schematically shows the relevant energy levels^{7,8,12,14} of SO_2^+ with the modified symmetry assignments of $\tilde{E}, \tilde{D}, \tilde{C}$ states by us. The excitations and the possible interactions among the electronic states were also given in Fig. 7, where ν_1 and ν_2 were the frequencies of photoionization laser and the photodissociation laser, respectively. The whole excitation and dissociation processes of SO_2^+ in the present study can be expressed as



E. Further discussion for the predissociation of \tilde{E} state

According to the PHOFEX spectrum in the range of 281–334 nm, we could not exclude the transitions of \tilde{E} ($\nu_1 = 0-2, \nu_2 = 1-4, \nu_3 = 0$) $\leftarrow \tilde{X}^2A_1(000)$, that is, there are two resonance band series. We must look for another repulsive state besides the α^2A_2 repulsive state. If we suppose at first that another repulsive state is the 2B_2 state and is called β^2B_2 , then the coupling between the β^2B_2 state and bound state 2B_2 or 2A_1 related $\tilde{E}, \tilde{D}, \tilde{C}$ could occur via electron–electron interaction (${}^2B_2 - {}^2B_2$) or electron vibration interaction (${}^2A_1 - {}^2B_2$) ($B_2 \times a_1 = B_2$). In this way, more than two series could be observed in the PHOFEX spectrum, and the continuum background in PHOFEX spectrum also can be explained by the direct excitation to the repulsive 2B_2 state from \tilde{X}^2A_1 . The problem is that the 2A_1 bound state related $\tilde{E}, \tilde{D}, \tilde{C}$ can also couple to β^2B_2 repulsive state ($A_1 \times b_2 = B_2$) to dissociate to $\text{SO}^+(X^2\Pi) + \text{O}(^3P_g)$, the related resonance band series should show in the PHOFEX spectrum, and we should observed three band series, but this is not true. However, it should be noticed that the favorable electron–vibration coupling of (${}^2B_2 - {}^2B_2$) generally is hard also to favor another electron–vibration coupling of (${}^2A_1 - {}^2B_2$), and may be the reason there only two band series observed. If we suppose a 2A_1 repulsive state, similar results will be deduced as noted earlier. Referring to the *ab initio* results, we prefer that the energy position of the 2B_2 bound state the higher than that of the 2A_1 bound state, so another repulsive state was selected as β^2B_2 . If so, the \tilde{E} state should possess 2B_2 symmetry and the leaving \tilde{C} state should possess the symmetry of 2A_1 . Finally we get the symmetry assignment to $\tilde{E}, \tilde{D}, \tilde{C}$, that is, $\tilde{E}^2B_2, \tilde{D}^2B_1$, and \tilde{C}^2A_1 . The above-presented discussion needs further study both in experiment and in theory.

IV. SUMMARY

By preparing SO_2^+ molecular ions via $[3+1]$ multiphoton ionization of the neutral SO_2 molecules at 380.85 nm, the photodissociation process and the symmetry of the excited states of SO_2^+ molecular ions has been investigated by measuring the photofragment SO^+ excitation spectrum in UV (282–332 nm) and visible (562–664 nm) wavelength. The PHOFEX spectrum in the UV range was assigned essentially to the $\text{SO}_2^+(\tilde{E}, \tilde{D}) \leftarrow \text{SO}_2^+(\tilde{X}^2A_1)$ transitions. The transitions from $\tilde{X}^2A_1(000)$ to the bend vibration levels of $\text{SO}_2^+(\tilde{D})$ were suggested. The lower ν_2 of $\sim 240 \text{ cm}^{-1}$ for \tilde{D} state, given by us, in comparison with ν_2 of $\sim 360 \text{ cm}^{-1}$ for \tilde{C} state, given by photoelectron spectrum (3, 4), means that the potential curve of the \tilde{D} state is not similar to other states along the bend vibrational coordinate. The symmetry of the \tilde{D} state of SO_2^+ was determined as \tilde{D}^2B_1 . Around \tilde{D} states there should be a repulsive state of symmetry α^2A_2 converging to the dissociation limit of $\text{SO}^+(X^2\Pi) + \text{O}(^3P_g)$, and the predissociation of $\text{SO}_2^+(\tilde{D})$ comes from the coupling between \tilde{D} and α^2A_2 repulsive state.

ACKNOWLEDGMENTS

Support from the National Natural Science Foundation of China (No. 20173053) and National Key Basic Research Special Foundation is gratefully acknowledged.

- ¹R. Schinke, *Photodissociation Dynamics* (Cambridge University Press, Cambridge, 1993).
- ²M. N. R. Ashfold and J. E. Baggott, *Molecular Photodissociation Dynamics* (Royal Society of Chemistry, London, 1987).
- ³L. Zhang, J. Chen, H. Xu, J. Dai, S. Liu, and X. Ma, J. Chem. Phys. **114**, 10768 (2001).
- ⁴W. G. Hwang, H. L. Kim, and M. S. Kim, J. Chem. Phys. **113**, 4153 (2000).
- ⁵D. Forney, C. B. Kellogg, W. E. Thompson, and M. E. Jacox, J. Chem. Phys. **113**, 86 (2000).
- ⁶M. Pons, O. Joubert, C. Matinet, J. Pelletier, J.-P. Panabiere, and A. Weill, Jpn. J. Appl. Phys., Part 1 **33**, 991 (1994).
- ⁷L. Wang, Y. T. Lee, and D. A. Shirley, J. Chem. Phys. **87**, 2489 (1987).
- ⁸D. M. P. Holland, M. A. MacDonald, M. A. Hayes, P. Baltzer, L. Karlsson, M. Lundqvist, B. Wannberg, W. von Niessen, Chem. Phys. **188**, 317 (1994).
- ⁹R. Basner, M. Schmid, H. Deutsch, V. Tarnovsky, A. Levin, and K. Becker, J. Chem. Phys. **103**, 211 (1995).
- ¹⁰G. Dujardin and S. Leach, J. Chem. Phys. **75**, 2521 (1981).
- ¹¹M. J. Weiss, T.-C. Hsieh, and G. G. Meisels, J. Chem. Phys. **71**, 567 (1979).
- ¹²T. F. Thomas, F. Dale, and J. F. Paulson, J. Chem. Phys. **84**, 1215 (1986).
- ¹³L. Zhang, L. Pei, J. Dai, T. Zhang, C. Chen, S. Yu, and X. Ma, Chem. Phys. Lett. **259**, 403 (1996).
- ¹⁴B. Xue, Y. Chen, and H.-L. Dai, J. Chem. Phys. **112**, 2210 (2000).
- ¹⁵G. Herzberg, *Electronic Spectra and Electronic Structures of Polyatomic Molecules* (Litton Educational, New York, 1966), pp. 140, 248, 445.
- ¹⁶I. H. Hillier and V. R. Saunders, Mol. Phys. **22**, 193 (1971).
- ¹⁷B. Brehm, J. H. D. Eland, R. Frey, and A. Kustler, Int. J. Mass Spectrom. Ion Processes **2**, 197 (1973).